JOURNAL OF AIRCRAFT
Vol. 45, No. 1, January–February 2008

Flight-Test Evaluation of the Tool for Analysis of Separation and Throughput

Liling Ren* and John-Paul B. Clarke†
Georgia Institute of Technology, Atlanta, Georgia 30332-0150

DOI: 10.2514/1.30198

The tool for analysis of separation and throughput has been developed to predict the range of possible trajectories of aircraft performing any given continuous descent arrival and thereby determine the minimum target spacing at a metering point, such that there is a high probability of no separation violations thereafter. The resulting reduced need for controller intervention is expected to facilitate the implementation of continuous descent arrival. This tool includes a fast-time Monte Carlo trajectory simulator and a theoretically rigorous separation analysis methodology based on the probabilistic characteristics of trajectories. The tool was used to determine the target spacing for a continuous descent arrival flight test conducted in September 2004 at Louisville International Airport. Results of the flight test indicate that the 15-n-mile target spacing yielded a conditional probability of 69.6% for the continuous descent arrival to runway 35L, very close to the predicted value of 68.6%; and an overall total probability of 81.7%, which is between the predicted values of 79.6% and 85.0% for the continuous descent arrival to runway 35L and 17R, respectively. The flight test demonstrated that, by using the tool as developed, continuous descent arrival can be efficiently implemented under moderate to moderately high traffic conditions, thereby achieving much needed environmental and economic benefits.

I. Introduction

WIDESPREAD implementation of the continuous descent arrival (CDA) requires the ability to predict the range of possible trajectories of different aircraft and thereby determine the minimum spacing at a metering point, such that there is a high probability of no separation violations during the remainder of the procedure, thus minimizing the need for controller intervention. This ability is also required for some of the proposed components of the Next Generation Air Transportation System (NextGen), such as trajectory based operations and superdensity operations [1].

In this paper, we briefly describe the tool for analysis of separation and throughput (TASAT) that has been developed for this purpose and present simulation analyses and postflight-test analyses that were performed with the tool in support of the successful CDA flight test conducted at Louisville International Airport (KSDF) in September 2004. These analyses serve as an evaluation of the TASAT.

In conventional arrival and approach procedures, air traffic controllers manage aircraft movement through vectoring, the process of giving ad hoc altitude, speed, and heading commands to pilots to adjust the spacing and sequence of aircraft for the final approach. The primary benefit of vectoring is that it gives controllers the flexibility that has, to date, been required to achieve a tightly spaced final approach queue, thereby maximizing runway throughput, which is essential to minimizing delays when there is high traffic demand. To manage spacing, aircraft are mostly directed to fly a step-down vertical profile with extended level segments at low altitude (see Fig. 1) and at low speed, often also with extended lateral flight paths. This results in flight time, noise, emissions, and fuel burn values that are significantly higher than their respective minimum possible values [2,3].

CDA has been shown by previous studies [2–4] to be a cost effective means of achieving near- and medium-term reductions in noise, emissions, fuel burn, and flight time during the arrival phase of flight. As seen in Fig. 2, level segments are ideally eliminated during a CDA resulting in a vertical profile that is higher than in a conventional arrival. The deceleration is also delayed, resulting in delayed flap extensions. Consequently, the engine thrust is significantly lower (mostly at the idle setting) and the aircraft speed is higher. Additionally, CDA would also follow a shorter lateral path. As such, the environmental and economic benefits can be achieved. The recent expanded use of area navigation (RNAV) arrivals provides new opportunities for CDA. In an RNAV CDA, parameters of the lateral path and vertical profile can be programmed in the Flight Management System (FMS) navigation database. This allows for the calculation of the descent profile by the FMS based on winds and aircraft weight, thus achieving the best performance for the given aircraft.

However, because of aircraft trajectory variations due to operational uncertainties, it is difficult for air traffic controllers to predict and maintain (without vectoring) adequate spacing between aircraft performing CDA without a decision support tool. When no such tool is available, as has been the case to date, controllers typically add arbitrarily large separation buffers, resulting in a negative impact on airport throughput [5], thereby limiting the implementation of CDA to a few airports and light traffic conditions.

In the conceptual framework that has been proposed for RNAV CDA procedure design and operation, the role of the controller is divided into four phases: merging and sequencing, spacing, monitoring, and intervention. An intermediate metering point (or simply metering point) connects the descent from cruise and the low-noise descent from this point to the runway. Target spacings, similar to the widely used miles in trail (MIT) restrictions, between consecutive aircraft are given for the metering point such that there is a desired probability that separation minima are ensured throughout the remainder of the procedure without the need for controller intervention. During the low-noise descent, controllers monitor the spacing between aircraft and intervene only if additional spacing is required to prevent separation violations. Additional spacing is achieved by changing the speed profile, vectoring the aircraft off the CDA path and returning them when proper spacing is reestablished by extending the downwind leg, or by sidestepping to an alternate runway if it is available for use.

This conceptual framework offers great flexibility, because the location of the metering point can be changed if warranted by traffic

Received 1 February 2007; revision received 2 September 2007; accepted for publication 2 September 2007.

*Research Engineer, Daniel Guggenheim School of Aerospace Engineering, 270 Ferst Drive NW. Senior Member AIAA.

†Associate Professor, Daniel Guggenheim School of Aerospace Engineering, 270 Ferst Drive NW. Associate Fellow AIAA.

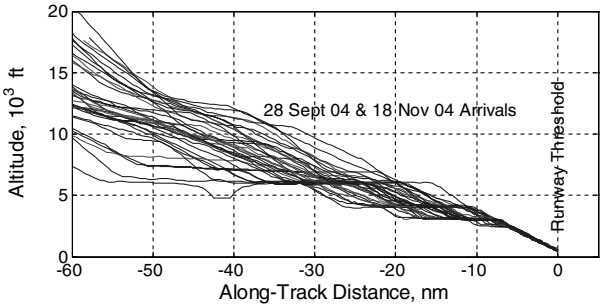

Fig. 1 Sample conventional vertical profile at KSDF.

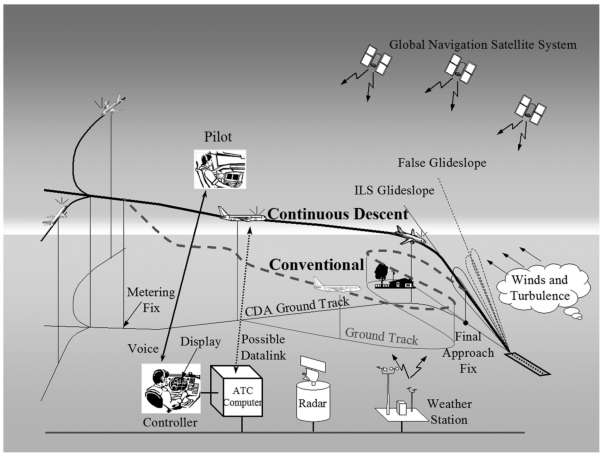

Fig. 2 CDA versus conventional arrival.

conditions. Ideally, the metering point should be as far away from the runway as possible, for example, before top of descent (TD), to maximize benefits. However, the farther the metering point is from the runway, the greater the target spacing must be, as larger buffers must be added to compensate for the larger trajectory variations that build up over longer distances. In lighter traffic, it can be moved farther away from the runway. In heavier traffic, it must be moved closer to the runway.

The remainder of this paper is organized as follows. The analysis tool to support the conceptual framework is briefly described in the next section, followed by a description of the KSDF CDA procedure design in Sec. III. The simulation analysis for the KSDF CDA using the aforementioned tool is presented in Sec. IV. Then the flight-test results are described in Sec. V, followed by a separation analysis using radar data collected during the flight test (Sec. VI). The conclusions are discussed in the last section.

II. Tool for Analysis of Separation and Throughput

The TASAT has two components. The first is a Monte Carlo simulation environment that has been developed to predict trajectory variations of aircraft conducting CDA. The second is a separation analysis methodology that has also been developed to determine target spacings required at the intermediate metering point. A brief description of the TASAT is given in this section to facilitate discussions that follow. Readers are referred to [6–8] for a complete description of this tool.

A. Monte Carlo Simulation Environment

For RNAV CDA, trajectory variations are generated in two ways. First, the flight path that is built by the onboard FMS varies from flight to flight in response to variations in operating conditions. Second, uncertainties encountered during the execution of the procedure cause deviations from the FMS-computed flight path.

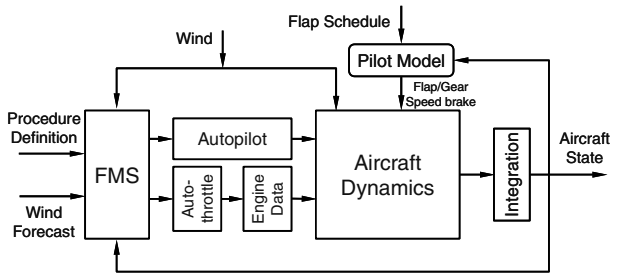

Fig. 3 Aircraft simulator block diagram.

Factors contributing to aircraft trajectory variations were identified as follows:

1) aircraft type: differences in aircraft design and dynamics;

2) CDA descent path logic: difference in aircraft equipage and design;

3) aircraft weight: variation due to demand and operational conditions;

4) pilot technique: variations among pilots and pilot response randomness;

5) weather conditions: predominantly variation in winds.

To ensure simulation accuracy, careful consideration was given to the modeling of each of these components. The central piece of the Monte Carlo simulation environment is a fast-time aircraft simulator. The structure of the aircraft simulator is shown in Fig. 3. The dynamics of the aircraft are determined using a point-mass model based on nonsteady-state equations of motion and thus more accurate in simulating wind effects than an ordinary point-mass model based on steady-state equations of motion. The model for each aircraft type was developed based on aerodynamic data and installed engine performance data provided by aircraft manufacturers. The autopilot, the autothrottle, and the FMS lateral navigation (LNAV) and vertical navigation (VNAV) capabilities are also modeled. Given the same CDA procedure design (such as that shown in Fig. 7), the FMS-computed VNAV path would vary with aircraft type and the flap schedule. These differences are captured by the FMS module in the aircraft simulator.

Because aircraft weight influences the FMS-computed VNAV path and aircraft performance, historical data collected from airline operations were used to model the distribution of the aircraft landing weight.

A pilot agent is included in the aircraft simulator to control the extension of flaps, landing gear, and speed brakes. For each aircraft type, the flap schedule in the corresponding aircraft operation manual [9], or one tailored to the given procedure, could be used. A pilot response delay model obtained from a previous human-in-the-loop simulation study [10] is included in the pilot agent.

Winds are the most significant single factor affecting aircraft trajectories. Winds are modeled using nominal profiles that reflect long-term statistical expectations and short-term variations that reflect wind changes between consecutive flights. A unique mode decomposition and autoregressive technique was developed to model wind variations between flights (see [7], Chapter 4). Specific wind models are developed using Aircraft Communications Addressing and Reporting System (ACARS) automated weather reports by commercial aircraft as archived by the National Oceanic and Atmospheric Administration [11].

The Monte Carlo simulation environment can be used to simulate a given procedure hundreds of times with different aircraft types and configurations under varying aircraft landing weights and wind conditions. Pilot response time is randomly generated for each of the control actions. Assuming there is no direct interaction between consecutive flights, each flight can then be simulated separately.

B. Separation Analysis Methodology

The distance versus time diagram for a specific pair of trajectories conducting the same CDA is depicted in Fig. 4. Assume that the leading trajectory and the trailing trajectory in the pair are

independent of each other. The minimum feasible spacing (the minimum spacing at the metering point that assures the separation minima for the specific trajectory pair during the descent to the runway) can be determined by moving the trailing trajectory in the direction parallel to the time axis (as indicated by the arrow) until the separation minima (shown by the dashed curve) are satisfied without additional spacing. If the actual spacing at the metering point is greater than the minimum feasible spacing for the specific trajectory pair, the procedure can be executed without interruption. The separation minima curve shown in the figure depicts the case where the separation minimum transitions from a larger radar separation minimum to a smaller radar separation minimum (or to a pairwise wake vortex separation minimum) as the aircraft get closer to the airport, for example, within 40 n mile, as shown by the kink on the curve.

It can be seen from Fig. 4 that the minimum feasible spacing depends on the separation minima, the location of the metering point, and the characteristics of both the leading and the trailing trajectories. Although in the figure the trailing trajectory is positioned such that it touches the separation minimum at the point when the leading aircraft is over the runway threshold, it is not necessarily always the case. The touch point could very well be at a location before that point. For a large sample of independent trajectory pairs, such as that obtained using the simulation described in the previous subsection, probability density functions (PDF) of the minimum feasible spacings could be estimated. Those probability densities are depicted schematically in Fig. 5. In the figure, only the PDF of aircraft sequences of type A leading type B and type B leading type A are shown. The difference between these two sequences as shown in the figure would occur when aircraft type B is from a weight class heavier than type A, in which different pairwise wake vortex separation minima would be used. The sequences with aircraft of the same type are omitted for the sake of simplicity.

For a selected target spacing, the probability of uninterrupted execution is the integral of the PDF from zero to the target spacing. Note that the probability is actually a conditional probability, as it is determined for the condition when the spacing at the metering point is exactly equal to the target spacing. To find out the proper target spacing, the vertical line in Fig. 5 can be shifted to the left or right (as indicated by the arrow) until the conditional probability is equal to a desired value (e.g., 70%). The method to determine the target spacing using this conditional probability is thus referred to as the conditional probability method.

In reality, neither controllers nor automation is this precise. The spacing at the metering point subject to a given target spacing would have a probability distribution itself as depicted by the thick gray curve (adjusted traffic) in Fig. 6. The thick black curve depicts the PDF of the spacing at the metering point when there is no special target spacing imposed (unadjusted traffic). With the PDF of spacings in adjusted traffic known, the total probability of uninterrupted procedure execution can be determined by computing the total probability for an infinitesimal slice of traffic and then integrating it from zero to infinity. The total probability for an infinitesimal slice of traffic (the patched small vertical strip in Fig. 6) is computed by multiplying the conditional probability at that point by the area of patched small vertical strip. The integration process is equivalent to finding the mean of conditional probabilities across all possible traffic spacings. Interested readers are referred to [7], Chapter 5 or [8] for the mathematical derivation of the total probability method. The method to determine the target spacing using the total probability is thus referred to as the total probability method.

The traffic throughput can be determined using the average time interval at the metering point. It is expected that given a target spacing at the metering point, the final spacing at the runway threshold would also be a probability distribution. Another specification of the traffic throughput, final separation buffer can thus be defined as the mean of final spacings minus the corresponding separation minima in effect at the runway threshold.

The separation analysis methodology has also been extended to the use of multiple sequence-specific target spacings. This has been discussed in great depth in the context of generic RNAV arrival procedures [8].

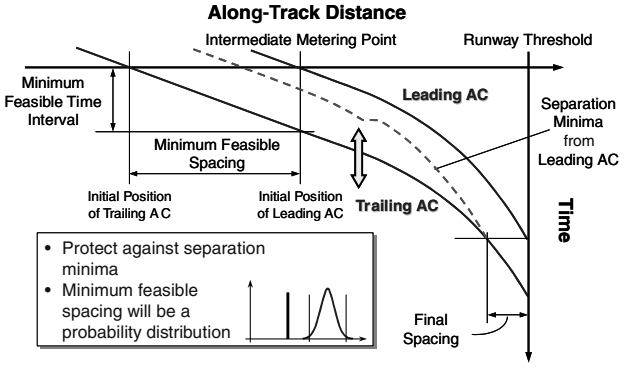

Fig. 4 Minimum feasible spacing.

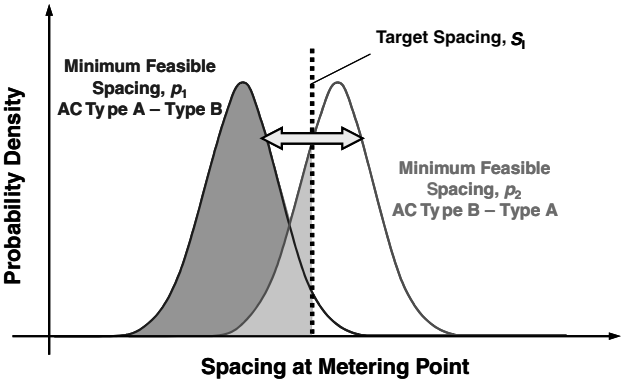

Fig. 5 Conditional probability method.

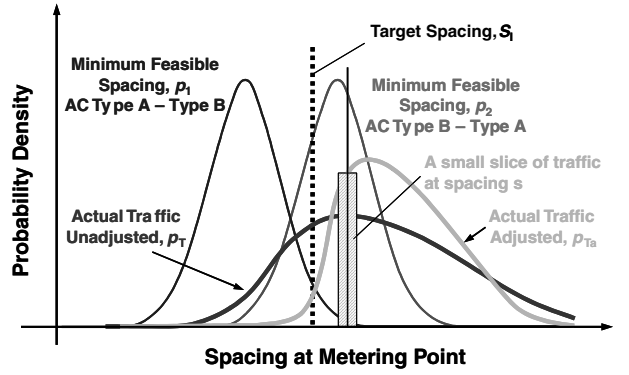

Fig. 6 Probability under adjusted traffic flow.

III. KSDF Procedure Design

A. Background

KSDF is the major hub for United Parcel Service (UPS) overnight package delivery operations. Because of the nature of the business, most UPS flight operations at KSDF occur during the night. Each weekday, about 100 jet transport aircraft (mostly UPS package freighters) land at KSDF in the 5-h period between 2200 and 0300 hrs, when residents are most sensitive to noise disturbance. Thus, KSDF was a perfect candidate site for conducting noise abatement procedure studies.

The two-week-long CDA flight test started on 14 September 2004 and involved 12–14 UPS B757-200 and B767-300 revenue flights each night. Aside from a demonstration of the effectiveness of the separation analysis methodology, objectives of the flight test also included a demonstration of the consistency of the procedure; measurement of the reductions in noise, fuel burn, emissions, and flight time; and the collection of data necessary to support the application for approval to perform the procedure on a regular basis [3].

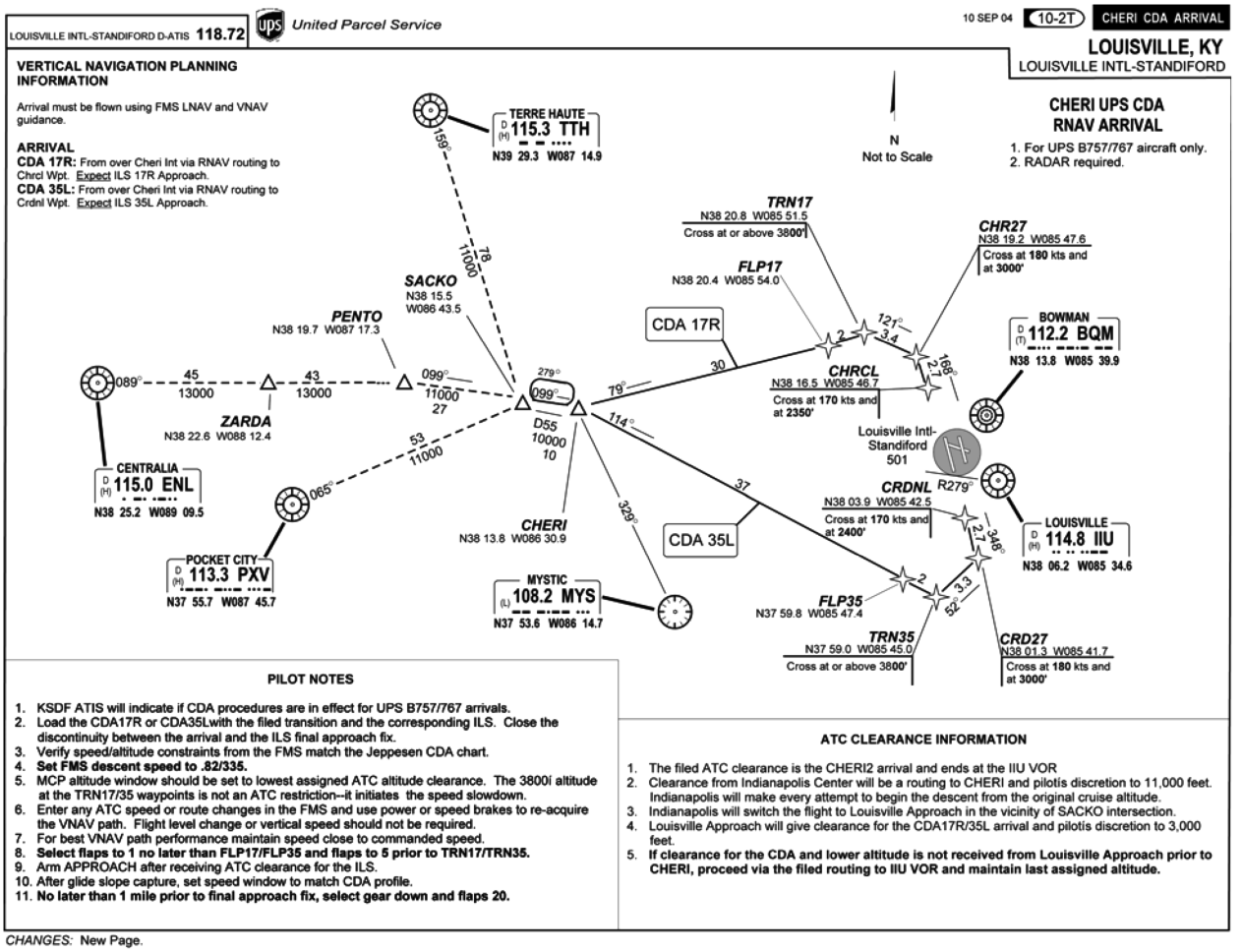

Fig. 7 Chart of the KSDF 2004 RNAV CDA.

B. KSDF CDA Procedure Design

The arrival chart for the CDA flown in the KSDF 2004 flight test is shown in Fig. 7. As noted in the top right corner of the chart, this is an RNAV CDA, in which the lateral and vertical flight paths are managed by the LNAV and VNAV functions, respectively, of the onboard FMS. The nominal lateral flight path was a routing via way points CENTRALIA, ZARDA, PENTO, SACKO, to CHERI and then to either runway 17R or 35L, depending on the prevailing winds on a given day.

The vertical profile was a continuous descent starting at the cruise altitude and defined by altitude and speed constraints given at way points TRN17, CHR27, and CHRCL for the CDA to runway 17R, or way points TRN35, CRD27, and CRDNL for the CDA to runway 35L. The characteristics of the altitude profile and speed profile are shown in Fig. 8. In this figure, the vertical lines indicate various feature points along the flight path. These points are identified either as fixed points or as computed points. The locations of fixed points were defined during the procedure design. The locations of computed points are computed by the FMS on board the aircraft. Along the altitude profile, two shallower segments are facilitated by the FMS to allow proper deceleration. The first one is at 10,000 ft and the second one is before the first vertical constraint at which the altitude is given. The FMS-computed VNAV free path segment, annotated in Fig. 8, is computed by the FMS based on the assumption that the aircraft will follow the speed profile at idle thrust. Ideally, the engine throttle would remain at idle from the TD until the aircraft is established on the final approach, when the instrument landing system (ILS) glide slope must be followed.

SACKO, which is a way point 10 n mile west of the terminal radar approach control (TRACON) boundary, was selected as the intermediate metering point. This way point is at −60.46 n mile along track distance for CDA to runway 35L and at −53.4 n mile for CDA to runway 17R. The along track distance is calculated along the CDA lateral path, with the positive sense pointing to the direction of flight and zero at the runway threshold. SACKO was selected as the metering point for two reasons: 1) to allow the aircraft hand off to occur before the speed transition from the descent speed of calibrated air speed (CAS) 335 kt to CAS 240 kt that occurs at 10,000 ft, and 2) to save more fuel.

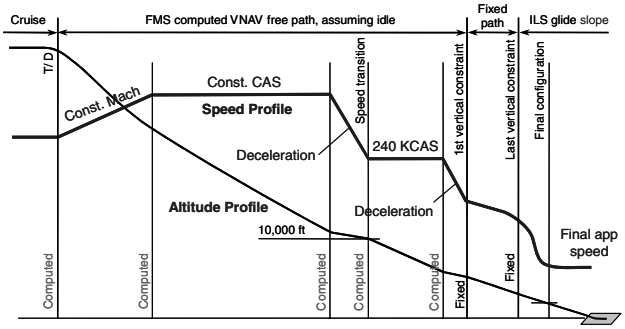

Fig. 8 Characteristics of the KSDF CDA vertical and speed profiles.

IV. Simulation Analysis

The TASAT was used to determine the target spacing used in the KSDF CDA flight test. The results of the corresponding simulation analysis are presented in this section. To be concise, only the results for the CDA to runway 35L are presented in detail.

Table 1 Vertical constraints for CDA to runway 35L

Way point	Distance, n mile	Altitude, ft	CAS, kt
TRN35	−11.45	Above 4000	——
CRD27	−8.14	3000	180
CRDNL	−5.79	2400	170
Runway	0	——	——

Table 2 Landing weight parameters, lb

	B757-200	B767-300
Mean	167,539	262,205
Standard deviation	11,000	18,000
Minimum	146,617	229,271
Maximum	194,534	298,183

A. Simulation Conditions

The altitude and speed constraints that define the vertical profile of the simulated procedure are listed in Table 1. The altitude constraint at way point TRN35 for the flight-test procedure is 200 ft lower than that for the simulated procedure. This change was introduced to assure proper capturing of the ILS glide slope from below. However, the separation analysis results presented here are valid for both procedures, because the lateral path and the speed profile remain the same. The descent speed was CAS 335 kt from cruise to 10,000 ft and CAS 240 kt (the FMS default value) from 10,000 ft to the point where the aircraft began decelerating to satisfy the first speed constraint.

Two aircraft types, B757-200 (B757) and B767-300 (B767), were simulated with random landing weights as defined in Table 2. The random pilot response model mentioned in Sec. II.A was used. The nominal wind profile (mean wind) and interflight wind variations were modeled using ACARS data reported between 2200 and 0300 hrs local standard time each day during the 6-month period from 10 February–12 August 2004.

B. Review of the Convergence of Density Estimation

Nonparametric probability density estimation is more appropriate for the PDF of minimum feasible spacings because less rigid assumptions need to be made about the true distribution. Suppose that X_i (where $i = 1, 2, \ldots, n$) denotes a sample of n independent and identically distributed observations. The corresponding kernel estimator of the spacing PDF $p(s)$ has the following form:

$$\hat{p}(s) = \frac{1}{nh_n} \sum_{i=1}^{n} K\left(\frac{s - X_i}{h_n}\right) \tag{1}$$

where $K(\,)$ is a kernel function with a window width h_n and

$$\begin{cases} \int_{-\infty}^{\infty} K(z)\,\mathrm{d}z = 1 \\ K(z) \geq 0 \end{cases} \tag{2}$$

The discrepancy between the estimated and the true PDF is often measured by the mean square error (MSE) and the mean integrated square error (MISE), defined by

$$\mathrm{MSE}\,[\hat{p}(s)] = E\{[\hat{p}(s) - p(s)]^2\} = \{E[\hat{p}(s)] - p(s)\}^2 + \mathrm{var}[\hat{p}(s)] \tag{3}$$

$$\begin{aligned} \mathrm{MISE}[\hat{p}] &= E\left\{\left(\int_{-\infty}^{\infty} [\hat{p}(s) - p(s)]^2\,\mathrm{d}s\right)\right\} \\ &= \int_{-\infty}^{\infty} \{E[\hat{p}(s)] - p(s)\}^2\,\mathrm{d}s + \int_{-\infty}^{\infty} \mathrm{var}[\hat{p}(s)]\,\mathrm{d}s \end{aligned} \tag{4}$$

For the kernel estimator, it can be obtained that [12]

$$E[\hat{p}(s)] = \int_{-\infty}^{\infty} \frac{1}{h_n} K\left(\frac{s - x}{h_n}\right) p(x)\,\mathrm{d}x \tag{5}$$

$$\begin{aligned} \mathrm{var}[\hat{p}(s)] = {} & \frac{1}{n} \int_{-\infty}^{\infty} \frac{1}{h_n^2} K\left(\frac{s - x}{h_n}\right)^2 p(x)\,\mathrm{d}x \\ & - \frac{1}{n}\left[\int_{-\infty}^{\infty} \frac{1}{h_n} K\left(\frac{s - x}{h_n}\right) p(x)\,\mathrm{d}x\right]^2 \end{aligned} \tag{6}$$

It can be seen from Eq. (5) that, for a given PDF to be estimated at s, the bias $E[\hat{p}(s)] - p(s)$ does not depend on the sample size, but depends only on the kernel function and window width. The variance does reduce as the sample size increases. In fact, assume that the kernel K could take negative as well as positive values and satisfies

$$\begin{cases} \int_{-\infty}^{\infty} |K(z)|\,\mathrm{d}z < \infty \\ \int_{-\infty}^{\infty} K(z)\,\mathrm{d}z = 1 \\ |tK(z)| \to 0 \quad \text{as } |z| \to \infty \end{cases} \tag{7}$$

Note that Eq. (7) is automatically satisfied by Eq. (2). Further, if the window width satisfies

$$h_n \to 0 \quad \text{and} \quad nh_n \to \infty \quad \text{as } n \to \infty \tag{8}$$

and if p is continuous at s, then [12]

$$\hat{p}(s) \to p(s) \quad \text{as } n \to \infty \tag{9}$$

This is to say that the kernel estimator defined by Eq. (1) is a consistent estimate of the true PDF under the conditions that the kernel satisfies Eq. (7), and that the window width approaches zero at a rate slower than the inverse of the sample size.

In practice, the PDF $p(s)$ of minimum feasible spacing can be viewed as being within the domain $[a, b]$. Suppose the domain is divided into m bins with the same width $2h_n$, and each of the bins is centered at t_i, where $i = 1, 2, \ldots, m$. The commonly used histogram estimator can be written as

$$\hat{p}(s) = \begin{cases} \frac{k_i}{2nh_n} & \text{for } (t_i - h_n) \leq s < (t_i + h_n) \\ 0 & \text{otherwise} \end{cases} \tag{10}$$

where k_i is the number of samples falling in the ith bin $[t_i - h_n, t_i + h_n)$.

The histogram estimator given in Eq. (10) is equivalent to a kernel estimator as defined in Eq. (1), with the following kernel function:

$$K\left(\frac{\tau - x}{h_n}\right) = \begin{cases} \frac{1}{2} & \text{if } \begin{cases} (t_i - h_n) \leq x < (t_i + h_n) \\ (t_i - h_n) \leq \tau < (t_i + h_n) \end{cases} \\ 0 & \text{otherwise} \end{cases} \tag{11}$$

Letting $z = (\tau - x)/h_n$, the aforementioned kernel function can be rewritten as

$$K(z) = \begin{cases} \frac{1}{2} & \text{if } \frac{t_i - h_n - x}{h_n} \leq z < \frac{t_i + h_n - x}{h_n} \\ 0 & \text{otherwise} \end{cases} \tag{12}$$

The kernel function given in Eq. (12) satisfies the conditions given in Eq. (7). Thus, the consistency conditions given in Eq. (8) apply to the histogram estimator. Under a more restrictive condition requiring $p(s)$ to have continuous derivatives up to order 3, Tapia and Thompson [13] explicitly prove these consistency conditions for the histogram estimator. However, the rate of convergence could be very slow. In most cases, it can only be analyzed approximately.

C. Monte Carlo Simulation Scheme

Based on the review presented in the previous subsection, the histogram estimator was used for the PDF of minimum feasible spacings. Because the purpose of the separation analysis is to

determine the proper target spacing, a bin width of 0.25 n mile was selected. The PDF shown in this paper are linearly interpolated between histogram estimates at bin centers. In this case, a moderately small bin size was selected to achieve some smoothing on the PDF estimate.

To make best use of the interflight wind variation model, flights are identified as leading flights or trailing flights. For each aircraft type under a given set of external conditions, an ensemble of 200 leading flights is simulated with the nominal wind profile, whereas an ensemble of 200 trailing flights is simulated with the nominal wind profile plus random interflight wind variations. Because the leading ensemble and the trailing ensemble are simulated independent of each other, a trajectory from the leading ensemble and a trajectory from the trailing ensemble form an arbitrary sample trajectory pair. Thus, for each aircraft type, a total number of 40,000 trajectory pairs can be obtained from 200 simulation runs for each of the two positions (i.e., leading or trailing). This is a very efficient simulation scheme for obtaining large numbers of trajectory pairs.

To verify that the selected number of simulation runs is sufficient, a convergence analysis was performed. This was done by gradually increasing the number of simulation runs for each position from 5–200, with an increment step size of 5 runs. The number of trajectory pairs was thus increased from 5^2 or 25 to 200^2 or 40,000. Note that the number of trajectory pairs increases nonlinearly because the number of trajectory pairs follows the square of the number of simulation runs.

The metrics used is the integrated square difference (ISD) between successive estimates based on a successively larger number of simulations runs, defined by

$$\mathrm{ISD}\,[\hat{p}_{n_k}] = \int_a^b [\hat{p}_{n_k}(s) - \hat{p}_{n_{k-1}}(s)]^2\,\mathrm{d}s \tag{13}$$

where the number of trajectory pairs $n_k = (5k)^2$, for $k = 2, 3, \ldots, 40$. The interval $[a, b] = [5, 25]$ in n mile. The ISD is defined analogously to the definition of MISE. The results of the PDF estimate of minimum feasible spacings for CDA to runway 35L are shown in Fig. 9. It is seen that the simulation converges well.

Following the Monte Carlo simulation scheme where, for each runway configuration, each aircraft is simulated 200 times in the leading position and 200 times in the trailing position, 1600 trajectories were simulated for the two aircraft types and two runway configurations.

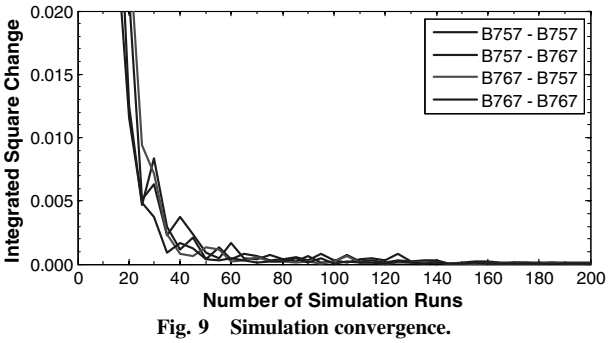

Fig. 9 Simulation convergence.

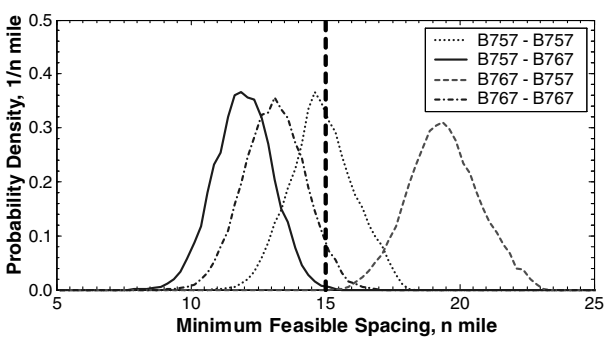

Fig. 10 Minimum feasible spacing at SACKO.

Table 3 Conditional probabilities and traffic throughputs for CDA to runway 35L

	Ideal case		$S_I = 15$ n mile		
Aircraft sequence	C_i, 1/h	$E(s_i)$, n mile	P_{Ri}, %	C_i, 1/h	β_{fi}, n mile
B757–B757	32.04	14.88	55.5	31.78	0.05
B757–B767	37.42	11.96	99.9	30.08	1.01
B767–B757	24.84	19.41	0.0	31.78	−1.30
B767–B767	34.24	13.11	95.2	30.08	0.62
Average	31.40	14.84	62.7	30.91	0.09

D. Minimum Feasible Spacing and Target Spacing

The PDF of minimum feasible spacings at SACKO were estimated from simulated trajectories per Instrument Flight Rules (IFR) separation minima. The results for runway 35L are shown in Fig. 10. Among the four aircraft sequences, the sequence of B767 leading B757 had the largest minimum feasible spacings. This was partially because this sequence has the largest final separation minimum among the four, 5 n mile, whereas the other three sequences require 4 n mile. Another factor was that the B757 aircraft, which was in the trailing position, had larger trajectory variations. This latter factor can also be seen by comparing the sequence of B757 leading B757 with the sequence of B767 leading B767.

Simulations were also done for various fixed extreme conditions such as minimum and maximum weights, zero wind, and 2σ wind. Based on the separation analysis results, and to adapt to the current practice of giving MIT restrictions in 5-n-mile increments, the research team determined that a target spacing of 15 n mile at SACKO would give an acceptable probability of uninterrupted execution. It is worth mentioning that a smaller increment would have allowed for a more optimal target spacing if that had been acceptable to the air traffic control.

E. Conditional Probability and Throughput

The throughput for an ideal case was examined first. The ideal case implies that trajectory variations were predicted precisely as they would happen, and that the spacing at the metering point for each aircraft pair was set exactly to the corresponding minimum feasible spacing for that aircraft pair. This means there would be no capacity loss in accommodating uninterrupted CDA execution, and that the final separation buffer would be nearly zero. Thus, throughputs for the ideal case indicate system capacity for the given aircraft mix and wind condition. For the ideal case, the traffic throughput C and the mean of spacing $E(s)$ at the metering point for each aircraft sequence i are listed in Table 3 as the group on the left. The average throughput values in the table were directly computed from the mean of the time

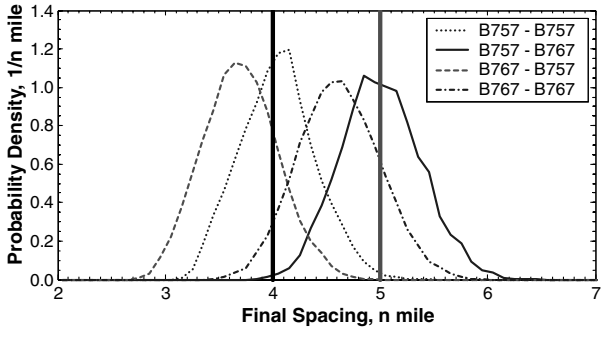

Fig. 11 Final spacing given 15 n mile at SACKO for the CDA to runway 35L.

Table 4 Number of CDA flights

		September										
Date		14	15	16	17	18	21	22	23	24	25	Total
35L	B757	6	7	——	5	8	6	7	7	——	8	54
	B767	6	5	——	6	6	6	6	5	——	6	46
17R	B757	——	——	6	——	——	——	——	——	6	——	12
	B767	——	——	6	——	——	——	——	1	6	——	13
Total		12	12	12	11	14	12	13	13	12	14	125

intervals at SACKO. The average throughput was 31.40 aircraft/h for the ideal case. Other items listed in the table are described later on.

The PDF of the final spacing for the target spacing of 15 n mile at the metering point for the CDA to runway 35L are shown in Fig. 11. The two vertical lines indicate the separation minima in effect at the runway threshold. The vertical line on the right is for the sequence of B767 leading B757, the vertical line on the left is for the other three aircraft sequences.

For the target spacing S_I of 15 n mile, conditional probabilities P_{Ri}, the throughputs C_i, and the final separation buffer β_{fi} for the four aircraft sequences are listed in Table 3 as the group on the right. The 15-n-mile target spacing yielded an average conditional probability P_R of 62.7% and an average final separation buffer β of 0.09 n mile. Notice that the conditional probability and final separation buffer varied drastically from aircraft sequence to aircraft sequence. The average throughput for a 15-n-mile target spacing was 30.91 aircraft/h, very close to the average throughput for the ideal case. Note that the averages in Table 3 were not weighted with any specific traffic mix. Thus, they are only applicable to scenarios where there is 50% of each aircraft type. For the CDA to runway 17R, the average conditional probability was 68.2% and the average throughput was 29.62 aircraft/h.

V. Flight-Test Results

The analyses of data collected during the KSDF 2004 CDA flight test are presented in this section to demonstrate the utility of the conceptual framework and to provide data to support the task of verifying the effectiveness of the Monte Carlo simulation environment and the separation analysis methodology in the section that follows.

A. Flight-Test Procedure

The KSDF CDA flight test began on Tuesday, 14 September and ended on Saturday, 25 September 2004. The flights involved in the test were all scheduled to arrive within the 1-h period between 0130 and 0230 hrs local daylight savings time each morning. A total of 125 flights performed the CDA. The numbers of CDA flown by each aircraft type to each runway are summarized in Table 4.

During the flight test, the Indianapolis Air Route Traffic Control Center (the center that surrounds the Louisville TRACON) was asked to make every effort to begin the descent from the original cruise altitude and to maintain a 15-n-mile spacing between aircraft. Aircraft were handed off to the TRACON at SACKO. The clearance from the Indianapolis center would be a routing to CHERI, with the pilot given discretion to descend to 11,000 ft. The TRACON would clear aircraft to proceed via the CDA to runway 35L (or 17R) and maintain 3000 ft. Before the way point FLP35 (or FLP17, refer to Fig. 7), the TRACON would issue another clearance to descend and maintain 3000 ft until established on the ILS localizer. This clearance served as a reminder to the pilot to prepare for the deceleration to 180 kt. The aircraft would then be handed off to the Louisville tower control and given clearance to land.

Pilots were required to select the CDA 35L (or the CDA 17R) procedure and the appropriate ILS procedure before the TD. During the descent, pilots were asked to keep the aircraft in FMS LNAV/VNAV path mode to best enable compliance with the altitude and speed constraints and the intended CDA profile. Minimum thrust or drag could be added as necessary to maintain the speed as close as possible to the VNAV target speed. Pilots were also required to select flaps 1 no later than FLP35 (or FLP17) and to select flaps 5 no later than TRN35 (or TRN17). These flap extension requirements were necessary to ensure proper deceleration before capturing the ILS localizer.

Should the spacing at the cruise altitude be sufficient and the descent profile properly managed, no vectoring would be necessary by either center or TRACON controllers during the descent. In this case, the engine throttle would likely remain at idle from TD until the aircraft is established on the final approach. Should the spacing at SACKO be projected to be less than the 15-n-mile target spacing, the center controller would use speed adjustment, lateral vectoring, or both to maintain a 15-n-mile spacing. If the 15-n-mile target spacing at SACKO were met, in most cases no vectoring by the TRACON controller would be needed. In any case, should the TRACON controller project that a separation violation were likely to occur, the aircraft would be vectored, or sent to the parallel runway.

Automated radar terminal system (ARTS) data during the flight test (two weeks, or 10 days) and after the flight test (18 days) were retrieved from the UPS surface management system. Flight data recorder (FDR) data were also collected. The analyses presented in this section and the next section are based on the aircraft trajectories extracted from these data.

B. CDA Ground Tracks

The ARTS ground tracks of the CDA flights and non-CDA flights are shown in Fig. 12. The solid thin tracks were normal CDA flights. The thick tracks (annotated with date and aircraft type) were CDA flights vectored for separation. The dotted thin tracks were non-CDA flights that had similar ground tracks as CDA flights. The thick B757 track on 23 September that joined the CDA lateral path after CHERI was not originally planned to fly CDA. Except for that flight, a total of six flights, or 4.84% of 124 CDA flights, were laterally vectored. Close examination revealed that the second thick B757 track on 23 September and the B757 on 18 September were vectored due to events not directly related to CDA.

C. Spacings at the Metering Point

The existing MIT restriction at the boundary between the Indianapolis center and the TRACON is 10 n mile. During the CDA flight test, a 15-n-mile target spacing was used. Traffic under the 10-n-mile MIT and the 15-n-mile target spacing are referred to as unadjusted and adjusted, respectively, to reflect the fact that the target spacing is higher than the existing MIT. Actual spacings at SACKO for 131 flight pairs from the unadjusted traffic and 60 flight pairs from the adjusted traffic were selected for the analysis. Other flight pairs were removed either because the spacing between a flight pair was larger than 30 n mile (considered as a gap in the arrival stream) or because another flight landed between the pair. The relative frequencies of these spacings are shown in Fig. 13 as bar charts.

Erlang PDF [14] were fit to the data to model traffic spacing. They are shown in Fig. 13 as curves. The Erlang distribution is selected because of its relation to the exponential distribution. The latter is often used to model intervals between independent arrivals. The ability of Erlang distribution to model the correlation between arrivals makes it an option to model traffic spacing that is subject to

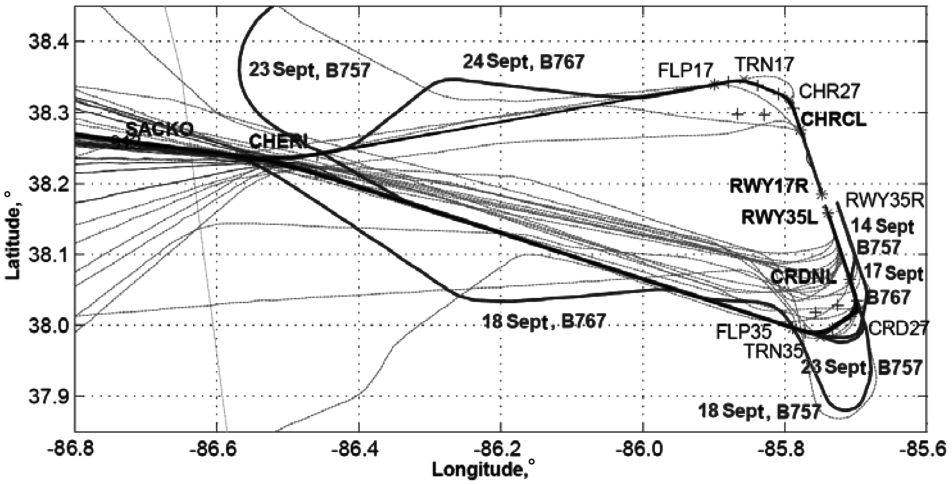

Fig. 12 KSDF 2004 CDA flight-test ground tracks.

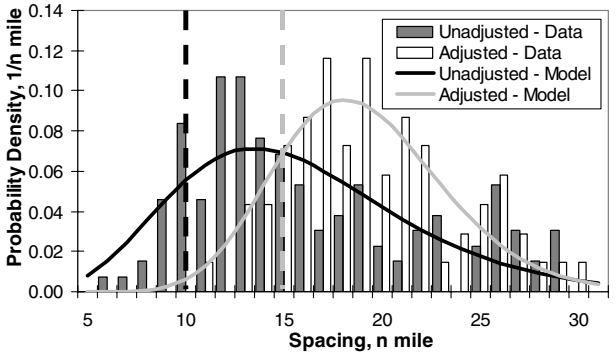

Fig. 13 Traffic spacing at SACKO.

intervention from the controller. The Kolmogorov–Smirnov (KS) test[‡] was performed to evaluate the goodness of fit of the Erlang models. The KS goodness of fit statistic (the maximum distance between the theoretical cumulative probability function (CDF) of the model and the empirical CDF of the data) for unadjusted traffic was 0.0920, whereas the critical value (for a sample size of 131) is 0.0935 at a significance level of 20%. The KS goodness of fit statistic for adjusted traffic was 0.0580, whereas the critical value (for a sample size of 69) is 0.1288 at a significance level of 20%. Thus, the Erlang models should not be rejected.

D. Observed Total Probability

Of the 69 flight pairs from the adjusted traffic, 60 involved at least one CDA flight. These 60 CDA flight pairs are analyzed next.

Twelve flight pairs had a spacing less than the target spacing of 15 n mile at the metering point. The trailing aircraft in four of these flight pairs were laterally vectored for separation. Speed reductions were applied to the trailing aircraft in two of the flight pairs before 10,000 ft. The speed of the leading aircraft (a non-CDA) was adjusted in one of the flight pairs. The crew of the trailing aircraft in two of the flight pairs accepted instructions from the controller to maintain visual separation; the final spacings were less than the IFR wake turbulence separation minima. This means nine, or 75% of these 12 flight pairs, were vectored one way or another, or were cleared to maintain visual separation. No controller intervention was observed for the remaining three pairs, and the separation minima were ensured with no need for vectoring. These three pairs illustrated that it is possible to perform an uninterrupted CDA even if the spacing at the metering point is below the recommended 15 n mile. It can be further speculated that the controller decided not to adjust the spacing between these three pairs because he or she was able to predict that the final spacing would be sufficient.

In two of the flight pairs that had a spacing greater than 15 n mile at SACKO, the crew accepted instructions from the controller to maintain visual separation; the final spacings were less than the IFR wake turbulence separation minima.

In short, the final spacing in 11 flight pairs, or 18.3% of the 60 CDA flight pairs, would have been less than the IFR wake turbulence separation minima if the controller had not intervened. This is equivalent to an overall total probability of 81.7%, regardless of runway configuration.

VI. Postflight-Test Analysis

The separation analysis methodology was applied to flight trajectories extracted from ARTS data. For this purpose, trajectories were selected based on how well the procedure was performed by each CDA flight, regardless of the actual spacing between consecutive flights at the metering point (i.e., SACKO). Some CDA flights were removed either because they were vectored (the trajectory would not reflect uninterrupted CDA execution), or because their VNAV paths were not properly computed due to FMS database issues, such as missing or inaccurate latitude/longitude, or speed/altitude constraints that were reported by some pilots when the procedure was loaded into the FMS before TD. The pilot test procedure calls for manually entering the missing or inaccurate data if they are encountered. There were cases where these missing data were not manually entered or were not entered as desired. These issues surfaced during the flight-test period because, for CDA, the whole process from FMS database update to pilot cockpit procedure was part of the test. Detailed discussion of this is beyond the scope of this paper. However, it was revealed after the flight test that these issues could be resolved through procedural means and thus would not be an issue in regular operation, as there would be sufficient time to ensure data accuracy. From the selected flight trajectories, CDA flight pairs were formed. These CDA flight pairs were not necessarily the consecutive flight pairs during the flight test. On rare occasions, a third flight might have landed between the pair of flights. For CDA to runway 35L, 73 flight pairs were formed. For CDA to runway 17R, 18 flight pairs were formed. The numbers of CDA flight pairs are listed in Table 5.

A. Minimum Feasible Spacing

The distance versus time diagram of CDA trajectories (to runway 35L) on 14 September are shown in Fig. 14. Trajectories on other days followed a similar pattern. All trajectories were aligned at SACKO to show the variation between flights. At any given point on the horizontal axis, the variation represents differences between flight times from SACKO to that point. At any given time on the

[‡]"NIST/SEMATECH e-Handbook of Statistical Methods" available online at http://www.itl.nist.gov/div898/handbook/ [retrieved 6 Aug. 2007].

Table 5 Number of CDA flight pairs

		September									
	Aircraft sequence	14	15	16	17	18	21	22	23	24	25	Subtotal
35L	B757–B757	2	4	——	1	3	4	2	2	——	2	20
	B757–B767	2	2	——	3	3	2	2	2	——	3	19
	B767–B757	1	1	——	2	2	1	2	1	——	3	13
	B767–B767	3	3	——	2	2	3	4	3	——	1	21
17R	B757–B757	——	——	4	——	——	——	——	——	3	——	7
	B757–B767	——	——	2	——	——	——	——	——	3	——	5
	B767–B757	——	——	1	——	——	——	——	——	2	——	3
	B767–B767	——	——	2	——	——	——	——	——	1	——	3

vertical axis, the variation represents differences between the aircraft locations. As expected, the larger the variations between flight trajectories were, the larger the minimum feasible spacings would be.

To obtain minimum feasible spacings, it is assumed that the trajectories would remain the same when spacings at the metering point between consecutive flights were adjusted slightly. Applying the process shown in Fig. 4, minimum feasible spacings at SACKO for the CDA flights listed in Table 5 can be obtained. The sample distribution for the CDA to runway 35L is shown in Fig. 15. Because of the small sample size, different aircraft sequences are not identified in the figure. The distribution thus indicates the weighted average based on the traffic mix listed in Table 5.

B. Conditional Probability

As seen from Fig. 15, in 69.9% of the cases the minimum feasible spacings were less than or equal to 15 n mile for the CDA to runway 35L. This is an estimate of the weighted average (by the traffic mix shown in Table 5) of conditional probabilities given a 15-n-mile target spacing at SACKO. For the CDA to runway 17R, the minimum feasible spacings were less than or equal to 15 n mile in 72.2% of the cases. The estimates of conditional probabilities are listed in Table 6, along with the simulation results that have already been presented.

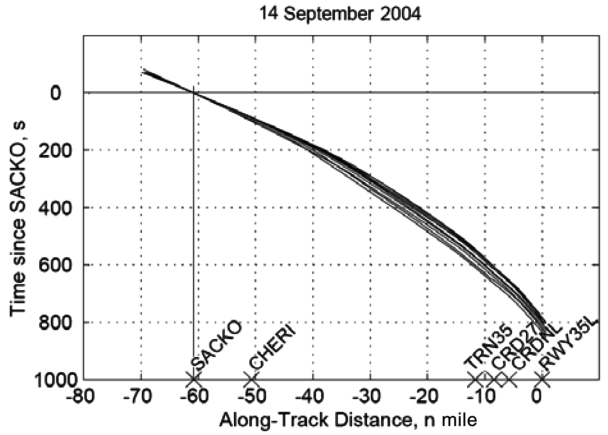

Fig. 14 14 September CDA trajectories.

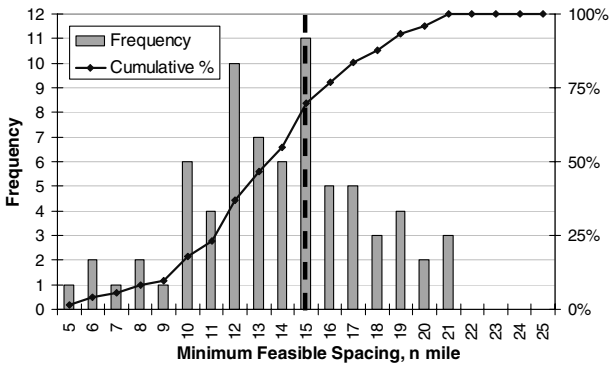

Fig. 15 Sample distribution of minimum feasible spacings for the CDA to runway 35L.

Table 6 Comparison of conditional probabilities given 15-n-mile target spacing

	Simulation results		
Procedure	Average	Weighted average	Flight-test results
CDA to 35L	62.7%	68.6%	69.9%
CDA to 17R	68.2%	72.5%	72.2%

Table 7 Estimated total probabilities assuming 50–50 traffic mix for CDA to runway 35L

Sequence	10-n-mile MIT	15-n-mile target spacing
B757–B757	52.0%	83.6%
B757–B767	72.1%	96.4%
B767–B757	25.5%	45.4%
B767–B767	64.3%	92.8%
Overall	53.5%	79.6%

In Table 6, the average values from the simulation were arithmetic averages, and the weighted average values were weighted by the traffic mix data shown in Table 5. It is seen that the weighted average values are very close to the flight-test results.

C. Total Probability

Using the Erlang distribution models of the spacings in the arrival stream under the 10-n-mile MIT and the 15-n-mile target spacing, the estimated total probabilities were obtained based on simulated trajectories described in Sec. IV. The results for CDA to runway 35L are listed in Table 7. It is seen that, by using a larger target spacing, the total probability has been greatly increased. Comparing Table 7 with Table 3, it is also seen that for the same target spacing of 15 n mile, the total probability is higher than the conditional probability. The estimated overall total probability for assuming 50–50 traffic mix for the CDA to runway 17R was 58.7% for the 10-n-mile MIT and 85.0% for the 15-n-mile target spacing.

It is seen that the overall total probability of 81.7% from the flight test (presented in Sec. V.D) and the simulated estimations are very close. The flight-test result is between the estimated overall total probabilities of 79.6% for the CDA to runway 35L and 85.0% for the CDA to runway 17R, respectively.

VII. Conclusions

The tool for analysis of separation and throughput has been developed to solve the problem of efficiently managing the spacing of continuous descent arrivals and includes a fast-time Monte Carlo aircraft trajectory simulation environment and a theoretically rigorous separation analysis methodology. The tool was used to

support the continuous descent arrival flight test conducted in September 2004 at Louisville International Airport. The flight-test results verified the accuracy of model predictions and proved the effectiveness of the separation analysis methodology. The flight test also demonstrated that continuous descent arrivals can be efficiently implemented under moderate to moderately high traffic conditions if the appropriate spacing at the metering point is determined. The tool is currently being used in arrival procedures development projects at a number of airports in the United States and Europe, including Nottingham East Midlands Airport [15] and London Gatwick Airport [16] in the United Kingdom, Los Angeles International Airport [17] and Hartsfield–Jackson Atlanta International Airport [18] in the United States. There is an ongoing effort to include more aircraft types in the aircraft simulator. The current version of the tool handles arrival traffic performing the same procedure. Work is underway to expand the tool to handle merging traffic.

Acknowledgments

This work was funded by the Federal Aviation Administration (FAA) under the PARTNER Project 4—Continuous Descent Approach. The authors would like to thank Frank Cardullo of Binghamton University; Kevin Elmer, Kwok-On Tong, and Joseph K. Wat of the Boeing Company; Nhut Ho of California State University, Northridge; Dannie Bennett, Sarah Johnson, David Senechal, and Andrew Willgruber of the FAA; Eric Feron of Georgia Institute of Technology; Charles Oman of Massachusetts Institute of Technology; David Williams of NASA; and Jeffery Firth, Robert Hilb, Stuart Lau, and James Walton of UPS for providing various data and sharing their valuable expertise in this research effort.

References

[1] "Concept of Operations for the Next Generation Air Transportation System," Ver. 2.0, Next Generation Air Transportation System Joint Planning and Development Office, Washington, D.C., June 2007.

[2] Clarke, J.-P. B., Ho, N. T., Ren, L., Brown, J. A., Elmer, K. R., Tong, K.-O., and Wat, J. K., "Continuous Descent Approach: Design and Flight Test for Louisville International Airport," *Journal of Aircraft*, Vol. 41, No. 5, 2004, pp. 1054–1066.

[3] Clarke, J.-P. B., Bennett, D., Elmer, K., Firth, J., Hilb, R., Ho, N., Johnson, S., Lau, S., Ren, L., Senechal, D., Sizov, N., Slattery, R., Tong, K., Walton, J., Willgruber, A., and Williams, D., "Development, Design, and Flight Test Evaluation of a Continuous Descent Approach Procedure for Nighttime Operation at Louisville International Airport," Massachusetts Institute of Technology, Report of the PARTNER CDA Development Team, Report PARTNER-COE-2006-02, Cambridge, MA, Jan. 2006.

[4] "The Noise Benefits Associated with Use of Continuous Descent Approach and Low Power/Low Drag Approach Procedures at Heathrow Airport," Civil Aviation Authority Paper 78006, London, April 1978.

[5] Erkelens, L. J. J., "Research into New Noise Abatement Procedures for the 21st Century," AIAA Paper 2000-4474, Aug. 2000.

[6] Ren, L., Ho, N. T., and Clarke, J.-P. B., "Workstation Based Fast-Time Aircraft Simulator for Noise Abatement Approach Procedure Study," AIAA Paper 2004-6503, Sept. 2004.

[7] Ren, L., "Modeling and Managing Separation for Noise Abatement Arrival Procedures," Sc.D. Thesis, Dept. of Aeronautics and Astronautics, Massachusetts Inst. of Technology, Cambridge, MA, Sept. 2006.

[8] Ren, L., and Clarke, J.-P. B., "A Separation Analysis Methodology for Designing Area Navigation Arrival Procedures," *Journal of Guidance, Control, and Dynamics*, Vol. 30, No. 5, 2007, pp. 1319-1330. doi:10.2514/1.27067. DOI:

[9] UPS B757/767 Aircraft Operating Manual, UPS Flight Publications, Document UPS33075, Louisville, KY, 2003.

[10] Ho, N. T., and Clarke, J.-P. B., "Mitigating Operational Aircraft Noise Impact by Leveraging on Automation Capability," AIAA Paper 2001-5239, 2001.

[11] "NOAA/ESRL/GSD Aircraft Data Web," [online database], http://acweb.fsl.noaa.gov/ [retrieved 28 Aug. 2007].

[12] Silverman, B. W., *Density Estimation for Statistics and Data Analysis*, Chapman and Hall, New York, 1986, pp. 34–71.

[13] Tapia, R. A., and Thompson, J. R., *Nonparametric Probability Density Estimation*, John Hopkins Univ. Press, Baltimore, MD, 1978, pp. 44–48.

[14] Larson, R. C., and Odoni, A. R., *Urban Operations Research*, Prentice–Hall, Englewood Cliffs, NJ, 1981, pp. 48–49.

[15] Reynolds, T. G., Ren, L., and Clarke, J.-P. B., "Advanced Noise Abatement Approach Activities at Nottingham East Midlands Airport, UK," FAA/EUROCONTRAL Paper 119, Washington, D.C., July 2007.

[16] Reynolds, T. G., Ren, L., Clarke, J.-P. B., Burke, A. S., and Green, M., "History, Development and Analysis of Noise Abatement Arrival Procedures for UK Airports," AIAA Paper 2005-7395, Sept. 2005.

[17] White, W., and Clarke, J.-P. B., "Details and Status of CDA Procedures at Los Angeles International Airport (LAX)," *CDA Workshop No. 3*, Georgia Inst. of Technology, Atlanta, GA, Sept. 2006.

[18] Clarke, J.-P. B., Brooks, J., Ren, L., Nagle, G., McClain, E., Boyce, G., Allerdice, J., Chambers, T., and Zondervan, D., "Flight Trials of CDA with Time-Based Metering at Atlanta International Airport," *AGIFORS Airline Operations 2007*, Airline Group of the International Federation of Operational Research Societies, Southlake, TX, May 2007.